Progress on Simulating the Initiation of Vacuum Insulator Flashover

M.P. Perkins, T.L. Houck, J.B. Javedani, G.E. Vogtlin, D.A. Goerz
Lawrence Livermore National Laboratory
7000 East Avenue
Livermore, CA 94550 USA

Abstract

Vacuum insulators are critical components in many pulsed power systems. The insulators separate the vacuum and non-vacuum regions, often under great stress due to high electric fields. The insulators will often flashover at the dielectric vacuum interface for electric field values much lower than for the bulk breakdown through the material. Better predictive models and computational tools are needed to enable insulator designs in a timely and inexpensive manner for advanced pulsed power systems. In this article we will discuss physics models that have been implemented in a PIC code to better understand the initiation of flashover.

The PIC code VORPAL [1] has been ran on the Linux cluster Hera at LLNL. Some of the important physics modules that have been implemented to this point will be discussed for simple angled insulators. These physics modules include field distortion due to the dielectric, field emission, secondary electron emission, insulator charging, and the effects of magnetic fields. In the future we will incorporate physics modules to investigate the effects of photoemission, electron stimulated desorption, and gas ionization. This work will lead to an improved understanding of flashover initiation and better computational tools for advanced insulator design.

I. INTRODUCTION

Investigating surface flashover has received much attention due to its importance in high voltage and pulsed power systems [2-10]. Although many of the mechanisms involved in surface flashover are believed to be understood, there are currently no reliable models to predict when insulators will fail or the optimum design under operational conditions [7].

One reason for not having a predictable model is due to the many different physical processes involved in flashover [2, 7, 8-10, 12]. The order of importance of the physical phenomena may also change for different operating conditions. To include all the physics phenomena a multi-physics particle in a cell (PIC) code such as VORPAL [1] is needed. We have implemented several physics modules in VORPAL and applied them to investigate the surface flashover problem.

Figure 1 shows pictures taken in the pulsed power lab at LLNL of a typical setup used to find the breakdown voltage of a +45° angled insulator as well as pictures demonstrating anode and cathode initiated flashover events [2]. In order to focus our attention on the physics involved in flashover, we will restrict ourselves in this discussion to slab like geometries where an insulator is placed between two electrodes of a planar parallel plate waveguide. In Sect. 2 we will begin by discussing how insulators affect the fields, insulator charging, field emission and secondary electrons from insulators. We will also discuss some modifications made to VORPAL that were implemented to help investigate this unique problem. In Sect. 3, we will apply these concepts to 0°, and ± 45° insulators. We will also apply an EM-pulse to a 45° insulator to demonstrate the effect of a magnetic field.

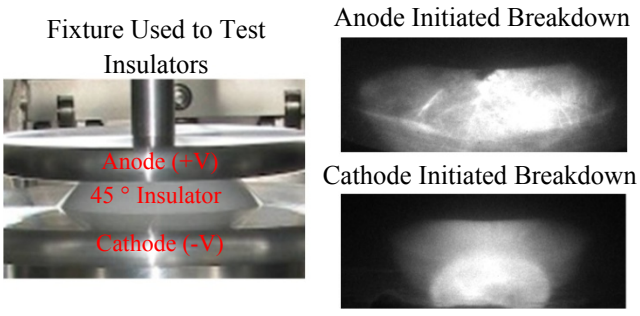

Figure 1. Pictures from [2] showing a typical setup to measure breakdown voltage as well as anode and cathode initiated breakdown across the surface of a +45° insulator.

This work performed under the auspices of the U.S. Department of Energy by Lawrence Livermore National Laboratory under Contract DE-AC52-07NA27344.
email: houck1@llnl.gov, perkins22@llnl.gov

Report Documentation Page

Form Approved
OMB No. 0704-0188

1. REPORT DATE	2. REPORT TYPE	3. DATES COVERED
JUN 2009	**N/A**	**-**

4. TITLE AND SUBTITLE	5a. CONTRACT NUMBER
Progress on Simulating the Initiation of Vacuum Insulator Flashover	5b. GRANT NUMBER
	5c. PROGRAM ELEMENT NUMBER
6. AUTHOR(S)	5d. PROJECT NUMBER
	5e. TASK NUMBER
	5f. WORK UNIT NUMBER
7. PERFORMING ORGANIZATION NAME(S) AND ADDRESS(ES) **Lawrence Livermore National Laboratory 7000 East Avenue Livermore, CA 94550 USA**	8. PERFORMING ORGANIZATION REPORT NUMBER
9. SPONSORING/MONITORING AGENCY NAME(S) AND ADDRESS(ES)	10. SPONSOR/MONITOR'S ACRONYM(S)
	11. SPONSOR/MONITOR'S REPORT NUMBER(S)

12. DISTRIBUTION/AVAILABILITY STATEMENT
Approved for public release, distribution unlimited

13. SUPPLEMENTARY NOTES
See also ADM002371. 2013 IEEE Pulsed Power Conference, Digest of Technical Papers 1976-2013, and Abstracts of the 2013 IEEE International Conference on Plasma Science. IEEE International Pulsed Power Conference (19th). Held in San Francisco, CA on 16-21 June 2013., The original document contains color images.

14. ABSTRACT
Vacuum insulators are critical components in many pulsed power systems. The insulators separate the vacuum and non-vacuum regions, often under great stress due to high electric fields. The insulators will often flashover at the dielectric vacuum interface for electric field values much lower than for the bulk breakdown through the material. Better predictive models and computational tools are needed to enable insulator designs in a timely and inexpensive manner for advanced pulsed power systems. In this article we will discuss physics models that have been implemented in a PIC code to better understand the initiation of flashover. The PIC code VORPAL [1] has been ran on the Linux cluster Hera at LLNL. Some of the important physics modules that have been implemented to this point will be discussed for simple angled insulators. These physics modules include field distortion due to the dielectric, field emission, secondary electron emission, insulator charging, and the effects of magnetic fields. In the future we will incorporate physics modules to investigate the effects of photoemission, electron stimulated desorption, and gas ionization. This work will lead to an improved understanding of flashover initiation and better computational tools for advanced insulator design.

15. SUBJECT TERMS

16. SECURITY CLASSIFICATION OF:			17. LIMITATION OF ABSTRACT	18. NUMBER OF PAGES	19a. NAME OF RESPONSIBLE PERSON
a. REPORT	b. ABSTRACT	c. THIS PAGE			
unclassified	**unclassified**	**unclassified**	**SAR**	**6**	

II. PHYSICS MODELED

Placing an angled insulator between two electrodes perturbs the electric field. Figure 2 shows how the y- and z-components are perturbed in the presence of a dielectric having a relative permittivity of 2.5 for ± 45° insulators. In the absence of the dielectric the field is polarized in the -y-direction and there is no z-component to the E-field. The boundaries are periodic in ±x, conductors in ±y, and absorbing in ±z. The dielectric is stair stepped in VORPAL for computing the EM-fields.

One can clearly see from this figure that for a -45° insulator an electron that is present near the cathode will be pulled up and into the insulator, whereas for a +45° insulator an electron will be pulled up and away. Because of the field enhancement near the cathode of a -45° insulator, the initiation mechanism is often assumed to be field emission of the cathode. Similarly, because of the field enhancement near the anode of a +45° insulator, the initiation mechanism is sometimes assumed to be field emission from the insulator [11]. As the grid size of the simulation is decreased, the field in these regions increases [13]. This will enhance field emission.

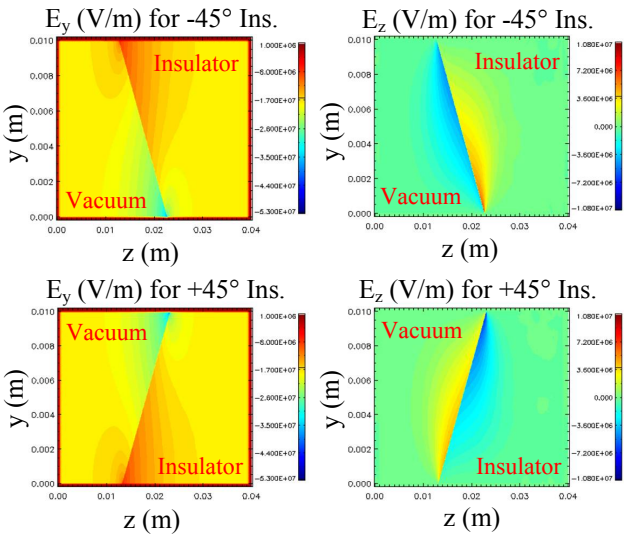

Figure 2. Steady state E-fields of a -45° and a +45° insulator with $\varepsilon_r = 2.5$.

In our simulations the Fowler-Nordheim field emission model of VORPAL has been applied for emission from both the cathode and the insulator. The field emission takes place from the true surface (not stair-stepped). A field enhancement factor β is used to multiply the E-field normal to the surface to take into account small perturbations in the surface that would require a much finer mesh to model [14].

One difference between field emission from the cathode and the insulator is that as electrons are removed from the insulator it will become positively charged. This is illustrated in Fig. 3. In this simulation an external static E-field in the -y-direction is applied. Field emission begins to occur, pulling electrons out of an insulator with $\varepsilon_r = 1.0$ (upper left) and causing it to begin charging (lower left). Long after the particles have finished emitting and left the simulation, a positive charge is retained on the surface of the insulator (right). In these figures the external field has been subtracted out.

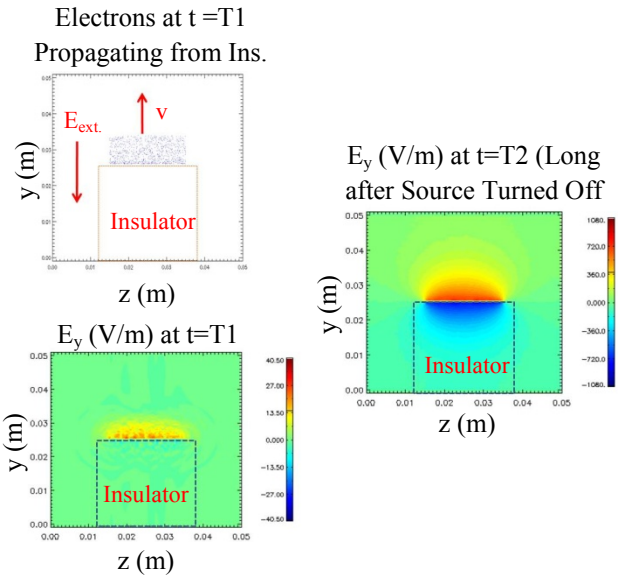

Figure 3. Field emission pulling electrons out of an insulator, causing it to charge positively. The E_y-field is shown with the external field subtracted out

After the electrons are introduced into the simulation via field emission, the EM-fields will cause them to move until they strike either an electrode or the insulator. When this happens they are absorbed and may create secondary electrons. VORPAL uses the model discussed in [15] to compute secondary electrons using the true surface (not stair- stepped). In [15] it is discussed that the number of secondary electrons produced depends on the energy of the incident electron and the incident angle from the normal of the surface (larger angle leads to more secondary electrons). The emitted electrons have a distribution in energy and angle.

Once again there is a difference between metals and insulators. For an insulator if the yield is zero, it must charge negatively. This is illustrated in Fig. 4 for a beam

of electrons propagating against a static E-field (upper left). The charge of the beam produces its own E-field (lower left). The number of macroparticles in the simulation (upper right) goes to zero after being absorbed by the insulator with ε_r = 1.0. Long after the particles have been absorbed the charge from the beam remains on the insulator surface, as indicated by the resultant E-field (lower right).

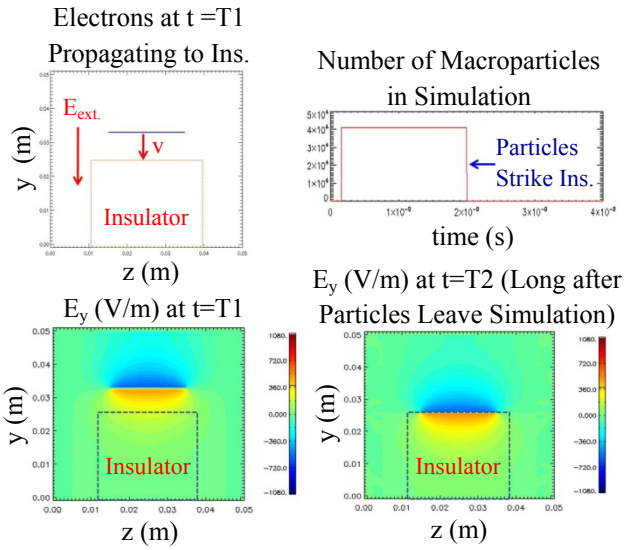

Figure 4. Illustration of insulator charge up when a beam of electrons is absorbed by an insulator, producing no secondary electrons. The E_y-field is shown with the external field subtracted out.

The numerical experiment discussed above is repeated, but this time the secondary electron yield is two. Figure 5 shows the secondary electrons produced (upper left) and being swept away from the insulator due to the external E-field. Note that there is now a distribution in angle and energies for the electrons. The surface of the insulator charges positively. One can see that the resultant positive E_y-field (lower left) that acts to pull the electrons back towards the surface, which is why the external E-field is needed. The number of macroparticles in the simulation (upper right) demonstrates the yield of two. The E-field long after the particles leave the simulation (lower right) is exactly opposite of the corresponding case shown in Fig. 4.

At the time of this publication, VORPAL does not have secondary electron information for insulators (just copper and stainless steel discussed in [15]). Thus, we are computing secondary electron information based on that of copper and stainless steel. In the future we may obtain this information for materials commonly used as insulators. Secondary electron yield information for some insulator materials seem to be similar to that of the metals being used. Unfortunately, measuring secondary electron data is more complicated than that of metals because of the surface charging phenomena [16, 17].

Because of the specific problems being investigated, we found it useful to make some modifications to the VORPAL source code for computing field emission and secondary electrons. For our problem we wanted to use

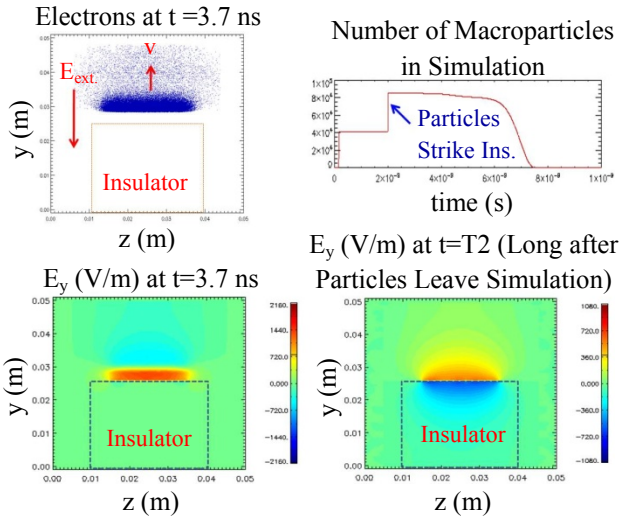

Figure 5. Illustration of insulator charge up when secondary electrons are created. The E_y-field is shown with the external field subtracted out.

constant weight macroparticles (i.e. number of electrons represented by a macroparticle the same) and allow for macroscopic field enhancement over the emission surface. This can be implemented by finding the amount of charge to emit using the E-field values over the local grid area to find the probability of emitting a macroparticle, as shown by Eq. (1) – Eq. (3).

$$Q = \int I dt = \int\int J_{FN} \cdot ds dt \approx J_{FN} \cdot \Delta s \int dt \quad (1)$$

$$NQ \approx J_{FN} \Delta s \Delta T = J_{FN} \Delta s * n \Delta t \quad (2)$$

$$n = \frac{NQ}{J_{FN} \Delta s \Delta t} \quad (3)$$

$$\text{if } \left({}^{1}/_{n} > \text{Random Number}(0,1)\right)$$
$$\text{then (Emit Macroparticle)}$$

In the above Eqs. Q is the charge, I the current, J_{NF} the Fowler-Nordheim surface current density (found using local E-field), Δs is the surface area of local grid element, N is the number of electrons in a macroparticle, ΔT the time since emitted from Δs, Δt is the time step, and n is the number of steps since emitting from Δs.

For secondary electrons, we would like them to be emitted only if they have an emission velocity great enough so that they do not return to the surface that emitted them in less one time step. To determine which electrons to emit we make use of Eqs. (4) and (5).

$$v_{Final} = 0 = v_{Initial} + a_{Normal} t_{Normal} \quad (4)$$

$$t_{Normal} = -\frac{v_{Initial}}{a_{Normal}}, a_{Normal} = \frac{qE_{Normal}}{m} \quad (5)$$

$$\text{if } (2 * t_{Normal} > \Delta t)$$
$$\text{then (Emit Macroparticle)}$$

In Eqs. (4) and (5) v_{Final} is the final velocity, $v_{Initial}$ is the initial velocity, a_{Normal} is the normal acceleration, $2 * t_{Normal}$ is the time to return to the surface, q is the charge, E_{Normal} is the normal electric field, and m is the mass.

III. APPLICATION TO DIFFERENT CONFIGURATIONS

Now that we have discussed some of the physics modules in VORPAL that are commonly believed to be important to surface flashover, we will apply them to some simple configurations. For the first numerical experiment we will apply a flat top EM pulse incident on an insulator with ε_r = 2.5. Then we allow for cathode field emission to take place near the insulator between 0.14 ns and 0.28 ns. The field emission does not take place until after the rising edge of the pulse passes the emission area. A static B-field is added to cancel out the B-field of the EM-pulse. As shown in Fig. 6 the electrons rapidly increase near the surface of the insulator. By the time the last electrons emitted from the cathode approach the anode, the number of macroparticles in the simulation has increased greatly (lower right).

The same simulation was repeated, but this time secondary electrons that have energies less than 0.4 eV were not allowed to emit from the insulator. As we can see in Fig. 7, the results are dramatically different. The number of macroparticles in the simulation do not increase as much near the anode (middle right), but there are still more secondary electrons being created than particles absorbed. This can be seen by looking at the E_z-field (bottom). There is still internal debate whether the low energy secondary electrons should be emitted from insulators. In Eq. (5) we sample E_{Normal}before any secondary electrons are emitted, but the removal of the electrons produces a surface charge on the insulator and hence alters E_{Normal} used to test our emit condition. This will be an area of future investigation.

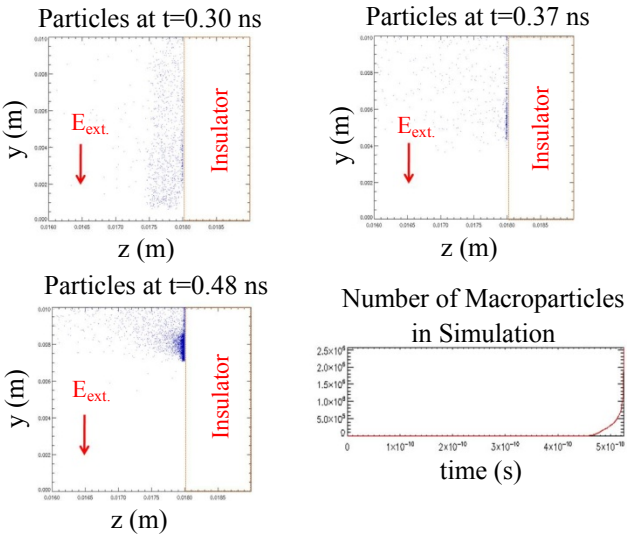

Figure 6. Cathode field emission takes place near the insulator surface. The number of macroparticles near the insulator increase greatly due to release of secondary electrons.

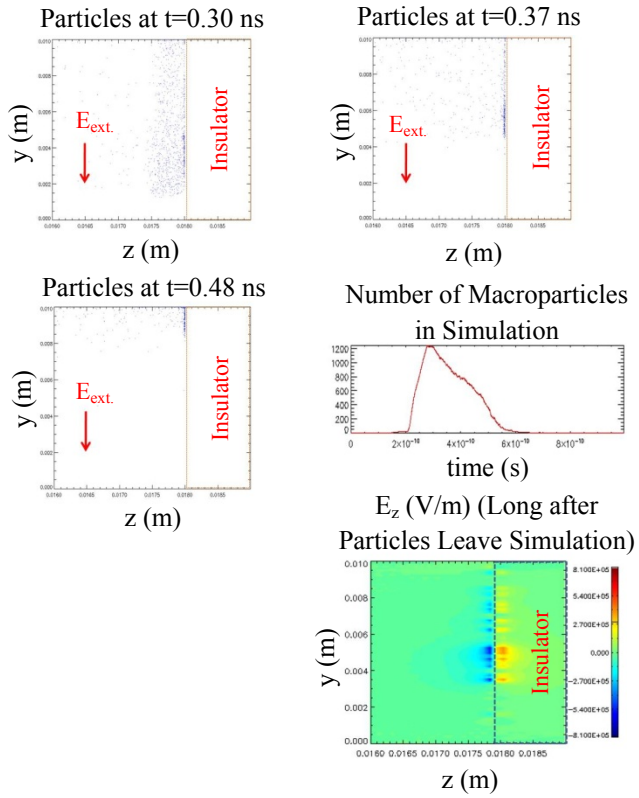

Figure 7. Cathode field emission takes place near the insulator surface. Secondary electrons with energies less than 0.4 eV are not emitted. The E_z-field indicates that there is a net gain of macroparticles from the insulator.

Next, the -45° insulator configuration that was shown in Fig. 2 (top) is investigated. We allow field emission from the cathode between 0.14 ns and 0.42 ns. Once again the field emission does not take place until after the rising edge of the flat top pulse passes the emission area and a static B-field is added to cancel out the B-field of the EM-pulse. The results are shown in Fig. 8. As can be seen as the insulator charges up, the E-field is such that it changes the trajectory of the electrons that have been field emitted. We can also see that there are many macroparticles that "stick" to the insulator and produce secondary electrons. The electrons stay in the simulation long after field emission has ended, as seen by the number of macroparticles in the simulation (bottom right). For this arrangement there was negligible difference between simulations that allowed secondary electrons with less than 0.4 eV to be emitted and those that didn't.

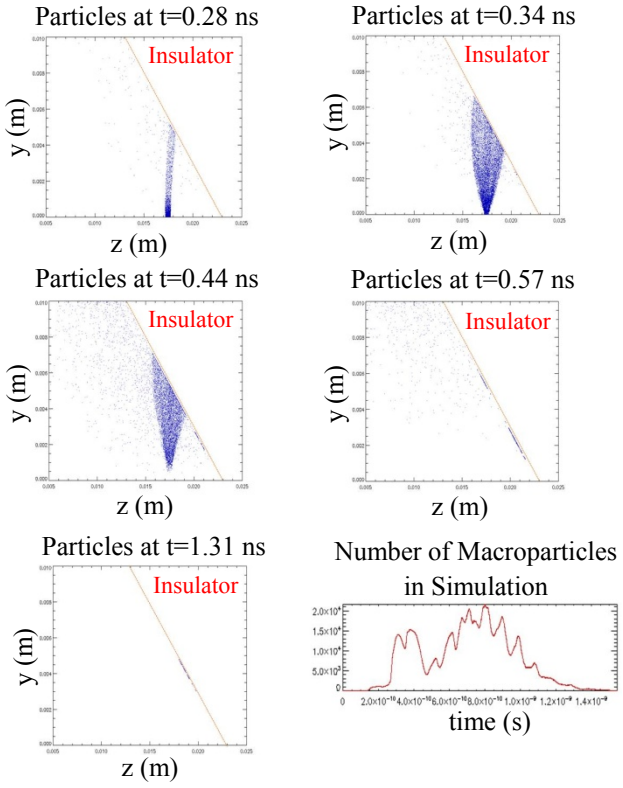

Figure 8. Cathode field emission takes place and the electrons strike the insulator producing secondary electrons. Macroparticles remain in the simulation long after field emission stops.

For the next setup we will use the +45° insulator arrangement that was shown in Fig. 2 (bottom). We allow field emission from the insulator to take place. A static B-field is added to cancel out the B-field of the flat top EM-pulse. The insulator begins to field emit near the anode triple junction due to the enhanced fields. The results are shown in Fig. 9. As the E-field increases the electrons begin to emit further down the insulator towards the cathode.

Finally, we investigate the effects from the B-field of the flat top EM-pulse propagating in the +z-direction incident on an insulator with $\varepsilon_r = 2.5$. The E_y, E_z, and B_x components of the EM-pulse are shown in Fig. 10 (first three figures). A field emission area on the cathode near the insulator begins emitting particles (light blue) as the rising edge of the pulse impinges on it (fourth figure). The B-field of the pulse causes these particles to bend toward the insulator. As these particles strike the anode, secondary electrons are created (red particles). The electrons then strike the insulator to produce secondary electrons from it (green particles). When the E-field becomes enhanced enough near the anode, field emission occurs from the insulator (dark blue particles). These results indicate that one side of the insulator will have electrons pushed towards it due to the B-field.

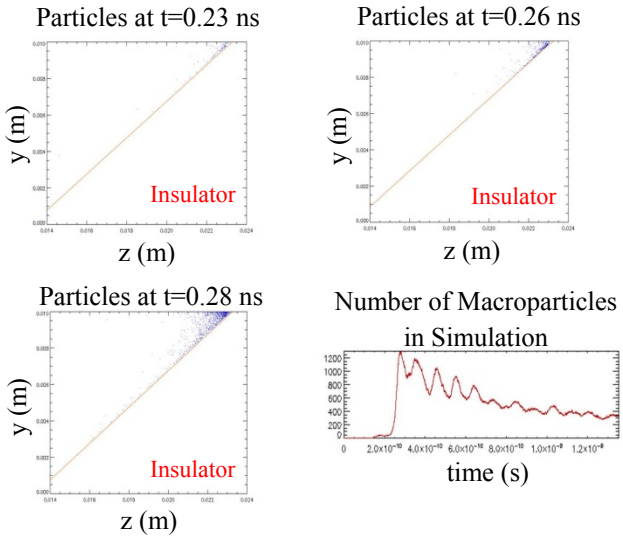

Figure 9. Insulator field emission takes place near the anode triple junction due to field enhancement. As the E-field increases electrons begin to emit further down the insulator towards the cathode.

IV. ACKNOWLEDGEMENTS

The authors would like to thank Peter Stoltz and Christine Roark of Tech-X Corporation for several helpful discussions about VORPAL. We would also like to thank Mike Ong, Laura Tully, and James McCarrick of LLNL for interesting discussions related to breakdown.

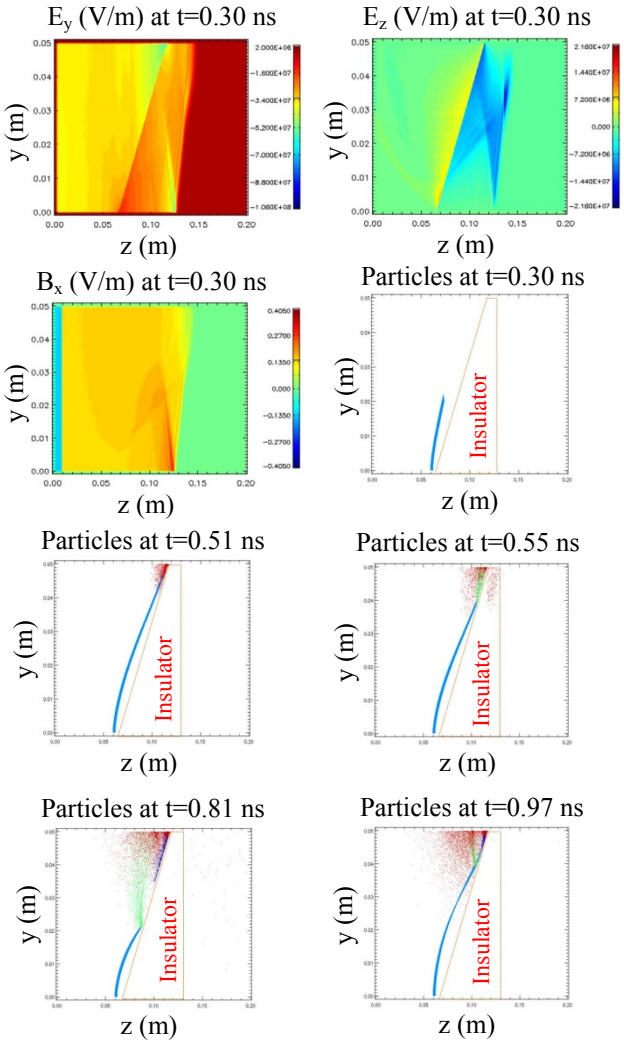

Figure 10. Flat top EM-pulse incident on insulator. The colored particles represent cathode field emission (light blue), anode secondary electrons (red) insulator secondary electrons (green) and insulator field emission (dark blue).

V. REFERENCES

[1] VORPAL available from Tech-X Corporation, 5621 Arapahoe Ave., Suite A, Boulder, CO, 80303, http://www.txcorp.com.

[2] J.B. Javedani, D.A. Goerz, T.L. Houck, E.J. Lauer, R.D. Speer, L.K. Tully, G.E. Vogtlin, A.D. White, "Understanding and Improving High Voltage Vacuum Insulators for Microsecond Pulses," UCRL-TR-228713, March 2007.

[3] T.L. Houck, D.A. Goerz, J.B. Javedani, E.J. Lauer, L.K. Tully, and G.E. Vogtlin, "Study of Vacuum Insulator Flashover for Pulse Lengths of Multi-Microseconds," Proc. Linear Accel. Conf., 2006, p. 610.

[4] J.B. Javedani, D.A. Goerz, T.L. Houck, E.J. Lauer, R.D. Speer, L.K. Tully, and G.E. Vogtlin, "Understanding High Voltage Vacuum Insulators for Microsecond Pulses," Proc. 16th IEEE Puls. Pow. Conf., 2007, p. 1836.

[5] G.E. Vogtlin, and J.E. Vernazza, "Vacuum Insulator Failure Measurements and Improvement," Proc. 7th IEEE Pulsed Power Conf., 1989, p. 808.

[6] J.B. Javedani, T.L. Houck, B.T. Kelly, D.A. Lahowe, M.D. Shirk, and D.A. Goerz, "UV Induced Insulator Flashover," Proc. 28th IEEE Int. Power Mod. and High Voltage Conf., 2008, p. 33.

[7] J.M. Wetzer, "Vacuum Insulator Flashover Mechanisms, Diagnostics and Design Implications," Proc. 17th Int. Symp. On Discharges and Electrical Insulation in Vacuum, 1996, p. 449.

[8] H.C. Miller, "Surface Flashover of Insulators," IEEE Trans. On Elec. Ins., Vol. 24, No. 5, pp. 765, Oct. 1989.

[9] N.S. Xu, R.V. Latham, B. Goddard, J. Tan, and W. Taylor, "Concurrent Optical and Electrical Observations of the 'Spontaneous' Surface Flashover of Solid Insulators in Vacuum," J. Phys. D: Appl Phys. 30, pp. 666, 1997.

[10] J.R. Harris et al. "Displacement Current and Surface Flashover," Applied Phys. Letters 91, 121504, p. 2007.

[11] W.A. Stygar et al. "Improved Design of a High-Voltage Vacuum-Insulator Interface," Phs. Rev. ST Accel. Beams 8, 050401, 2005.

[12] A.A. Neuber, M. Butcher, H. Krompholtz, L.L. Hatfield, M. Kristiansen, "The Role of Outgassing in Surface Flashover Under Vacuum," IEEE Trans. Plasma Science, pp. 1593, Oct. 2000.

[13] L.K. Tully, A.D. White, D.A. Goerz, J.B. Javedani, and T.L. Houck, "Electrostatic Modeling of Vacuum Insulator Triple Junctions," Proc. 16th IEEE Pulsed Power Conf., 2007, p. 1195.

[14] Y.Feng, J.P. Verboncoeur, and M.C. Lin, "Solution for Space Charge Limited Field Emission Current Densities with Injection Velocity and Geometric Effects Corrections," Physics of Plasmas 15, 043301, 2008.

[15] M.A. Furman and M.T.F. Pivi, "Probabilistic Model for the Simulation of Secondary Electron Emission," Phys. Rev. ST Accel. Beams 5, 124404, 2002.

[16] J. Cazaux, "e-Induced Secondary Electron Emission Yield of Insulators and Charging Effects," Nuclear Inst. And Methods in Phys. Res. Sec. B, pp. 307, 2006.

[17] L.L. Hatfield and E.R. Boerwinkle, "Secondary Electron Emission from a Thin Coating on Lucite and Lexan Substrates," Proc. Elec. Ins. and Dielectric Phenomena, 1989, p. 414.